# Altered Ligand Specificity by Protonation in the Ligand Binding Domain of Cyclic Nucleotide-Gated Channels†

Sharona E. Gordon, John C. Oakley, Michael D. Varnum, and William N. Zagotta*

*Department of Physiology and Biophysics, Howard Hughes Medical Institute, University of Washington, Box 357290, Seattle, Washington 98195-7290*

*Received November 2, 1995; Revised Manuscript Received February 5, 1996*⊗

ABSTRACT: Cyclic nucleotide-gated (CNG) ion channels are the critical mediators between the second messengers of sensory transduction and the cell's membrane potential. The photoreceptor CNG channels are activated by the direct binding of cGMP but can also be activated to a much lesser extent by cAMP. In rod CNG channels expressed in *Xenopus* oocytes, we demonstrate two types of potentiation by protons. One type potentiated cGMP-bound and cAMP-bound channels to the same extent, while another potentiated only cAMP-bound channels. Both types of potentiation could be described by a mechanism in which protons bound primarily to the channel open configuration. The potentiation specific to cAMP-bound channels could be accounted for by protonation of aspartic acid 604 (D604). It is the unfavorable electrostatic interaction between the carboxylate of D604 and the purine ring of cAMP that accounts for the normally poor activation of the channels by cAMP. Protonation at this site removed the unfavorable interaction and allowed cAMP to act as nearly a full agonist. Protonation of a second amino acid, H468, contributed to the nucleotide-nonspecific potentiation and is likely to be an element of the channel gating assembly. Protons potentiate native rod channels less than channels formed from subunit 1. In heteromultimeric channels formed by coexpressing subunit 1 with subunit 2, we found a similar attenuation of potentiation. The absence of protonatable amino acids in subunit 2 at positions corresponding to H468 and D604 can explain the reduced effects of pH on native channels.

Nonselective cation channels in rod photoreceptors link the photon-initiated enzyme cascade to the cell's membrane potential [reviewed in Lagnado and Baylor (1992)]. The chemical result of the enzyme cascade, hydrolysis of cGMP, is directly sensed by the channels, which contain a cyclic nucleotide-binding domain on each subunit. Although cGMP is the physiological regulator of the rod photoreceptor channel *in vivo*, it can be activated to a lesser extent by other cyclic nucleotides. Cyclic AMP is a partial agonist of the channels; in channels expressed from subunit 1 in *Xenopus* oocytes, a saturating concentration of cAMP activates only 1% of the channels activated by cGMP. The initial binding of cAMP is comparable to that of cGMP, but cAMP is much less able to promote channel opening once bound (Gordon & Zagotta, 1995a).

Discrimination among cyclic nucleotides is an essential feature of other cyclic nucleotide-regulated proteins as well. The cyclic nucleotide-binding domain of the cyclic nucleotide-gated (CNG) channels shares structural homology with such diverse proteins as cGMP- and cAMP-activated protein kinases and the bacterial catabolite gene activator protein (Su et al., 1995; Takio et al., 1984; Weber & Steitz, 1987). The cyclic nucleotide specificities of these proteins, however, vary widely. For example, the catfish olfactory channel is activated equally well by cAMP and cGMP (Goulding et al., 1992), while saturating cAMP activates expressed rod channels to only 1% of the level activated by saturating cGMP. In addition, while the rat olfactory channel subunit 1 exhibits appreciable selectivity for cGMP over cAMP, channels formed by coexpression of subunit 1 and subunit 2 are nearly equally selective for cGMP and cAMP (Bradley et al., 1994; Liman & Buck, 1994).

Recently, an amino acid within the cyclic nucleotide-binding domain has been identified as a major determinant of agonist efficacy and specificity (Varnum et al., 1995). Mutation of a single residue, aspartic acid 604 (D604) in the rod channel, had profound effects on the agonist specificity of the channel, and could transform it from a channel activated primarily by cGMP to one activated primarily by cAMP. D604 was proposed to mediate this discrimination by forming a pair of hydrogen bonds specifically with the guanine ring of cGMP. Rather than affecting the initial binding of cyclic nucleotides, mutations of D604 altered the ability of a given cyclic nucleotide to promote the allosteric transition from the closed to the open configuration. Thus, the interaction between D604 and the cyclic nucleotide purine ring is thought to occur as part of channel opening. Here we report that protonation of D604 specifically potentiated activation of the channels by cAMP. The cAMP-specific potentiation appeared to result from an attenuation of the unfavorable interaction between the D604 carboxylate group and the unshared electrons at N1 of cAMP. These results emphasize the importance of the interaction of cyclic nucleotides with D604 in determination of the free energy of the allosteric transition. A second, nucleotide-nonspecific type of potentiation resulted from protonation of H468, suggesting that H468 is associated with the channel gating process.

† This work was supported by a grant from the National Eye Institute (EY10329 to W.N.Z.) and the Human Frontier Science Program. W.N.Z. is an Investigator and S.E.G. and M.D.V. are Associates of the Howard Hughes Medical Institute.

⊗ Abstract published in *Advance ACS Abstracts,* March 15, 1996.

0006-2960/96/0435-3994$12.00/0 

## MATERIALS AND METHODS

The bovine rod channel subunit 1 cDNA was isolated as previously described (Gordon & Zagotta, 1995a). Channels identical to the published sequence (Kaupp et al., 1989) were used in addition to channels that contained an alanine to valine substitution at position 483 (A483V). The apparent affinity of A483V channels was slightly lower than that of wild type, but the effects of protons were the same for A483V and wild type (see Figure 3). The cDNA clone for the human photoreceptor subunit 2 (Chen et al., 1993) was kindly provided by the laboratory of K.-W. Yau (The Johns Hopkins School of Medicine, Baltimore, MD). This cDNA was subcloned into a high-expression vector, kindly provided by E. R. Liman, that contained the untranslated sequences of the *Xenopus* $\beta$-globin gene (Liman et al., 1992). Mutant cDNAs were constructed as described previously (Gordon & Zagotta, 1995a) by a method involving polymerase chain reaction (PCR) and were verified by sequence analysis. RNA was transcribed *in vitro* and injected into oocytes from *Xenopus laevis* as previously described (Zagotta et al., 1989).

Current recordings were made using the inside-out configuration of the patch−clamp technique (Hamill et al., 1981). All currents shown are difference currents, in which the current at the corresponding voltage, but in the absence of cyclic nucleotides, has been subtracted. The slight droop in some of the records reflects ion depletion that occurred when very large currents were passed (Zimmerman et al., 1988). Because the gating kinetics were very fast at high cyclic nucleotide concentrations, we were able to minimize the effects of ion depletion by measuring these currents within 2 ms of the voltage jump to +100 mV. Steady-state measurements of currents in response to subsaturating cyclic nucleotide concentrations were made at 40−80 ms, because of the slower gating kinetics observed in these cases. Currents were acquired and analyzed as previously described (Gordon & Zagotta, 1995a,b), with filtering at 2 kHz (−3 dB; eight-pole, low-pass Bessel filter) and digitization at 10 kHz. For experiments to study the effects of $Ni^{2+}$ potentiation in detail, the bath solution contained 130 mM NaCl, 3 mM HEPES, and either 0.2 mM ethylenediaminetetraacetic acid (EDTA) or 10 $\mu$M $Ni^{2+}$ (pH 7.2), and the extracellular solution contained 130 mM NaCl, 3 mM HEPES, 0.2 mM EDTA, and 0.5 mM niflumic acid (pH 7.2). Niflumic acid was used to block native oocyte channels and did not alter measured CNG channel properties. For the pH experiments, 2-(*N*-morpholino)ethanesulfonic acid (MES) was used instead of HEPES to more effectively buffer over the pH range used. For these experiments, the bath solution contained 130 mM NaCl, 3 mM MES, 0.2 mM EDTA, and the proton concentration indicated in each of the figures, and the extracellular solution contained 130 mM NaCl, 3 mM MES, 0.2 mM EDTA, and 0.5 mM niflumic acid (pH 7.2). To measure the maximum activatable current in a patch ($I_{max}$), the following solution was used: 130 mM NaCl, 3 mM MES, a saturating concentration of cGMP (8 or 2 mM), and either 1 or 10 $\mu$M $Ni^{2+}$ (Gordon & Zagotta, 1995a) (pH 7.2 or 5.0). Cyclic nucleotides were added to the bath solution, as indicated in the figure legends. All recordings were performed at room temperature (18−22 °C).

Determination of apparent affinity for cGMP was made by fitting dose−response curves with the Hill equation:

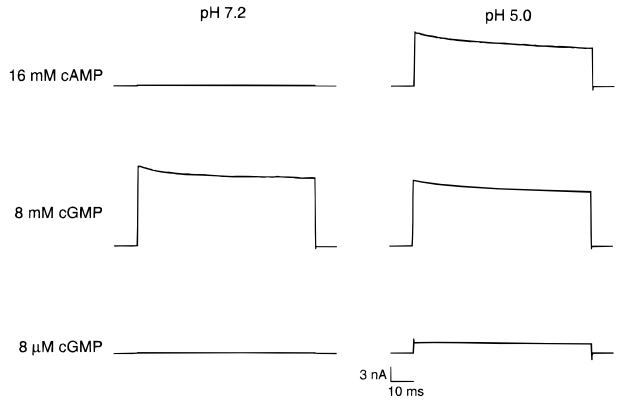


FIGURE 1: Potentiation of the rod CNG channel by protons. Currents were recorded in response to voltage jumps from a holding potential of 0 to +100 mV. The scale bar in the lower right corner applies to all parts of the figure. Cyclic nucleotide concentration and bath pH were as labeled in the figure.

$$I = I_{sat}\frac{[cGMP]^n}{K_{1/2}{}^n + [cGMP]^n}$$

in which $I_{sat}$ is the maximum current for the patch at saturating cGMP, $K_{1/2}$ is the concentration of cGMP that activates one-half of the channels activated by saturating cGMP, at a given pH, and $n$ is the Hill coefficient.

## RESULTS

We have studied the effects of protonation in rod CNG channels expressed from subunit 1 in *Xenopus* oocytes. Cyclic nucleotides were applied to the cytoplasmic face of excised inside-out patches from these oocytes. Currents were elicited by application of voltage steps from a holding potential of 0 to +100 mV, and the leak current in the absence of cyclic nucleotides was subtracted. cAMP, a partial agonist of the rod channels, activated approximately 1% of the channels activated by cGMP (compare at pH 7.2, 8 mM cGMP to 16 mM cAMP, Figure 1). As the single-channel conductance of cAMP- and cGMP-bound channels are comparable (Ildefonse et al., 1992), and addition of more cAMP does not further increase the current, differences in ion permeation or ligand binding are not likely to account for the disparate efficacies of cGMP and cAMP. Rather, the primary difference between activation of the channels by cGMP and cAMP has been suggested to lie in the ability of the cyclic nucleotides to promote the allosteric conformational change from the closed to the open configuration (Gordon & Zagotta, 1995b). Even though cAMP initially binds to the channels nearly as well as does cGMP, once bound, it is much less able to induce channel opening. Therefore, even at saturating cAMP concentrations, the current measured is quite small.

Increasing the proton concentration dramatically potentiated activation of the channels by both cyclic nucleotides. At pH 5.0, the current in response to saturating cAMP increased about 100-fold (Figure 1, top). The fraction of current activated by saturating cAMP, with respect to saturating cGMP, increased from 0.00624 (±0.00297, $N$ = 6; mean ± standard deviation) at pH 7.2 to 0.814 (±0.018, $N$ = 5) at pH 5.0. Potentiation by protons was also observed with a low concentration of cGMP (Figure 1, bottom). The current activated by 8 $\mu$M cGMP increased 21.1-fold (±7.3,

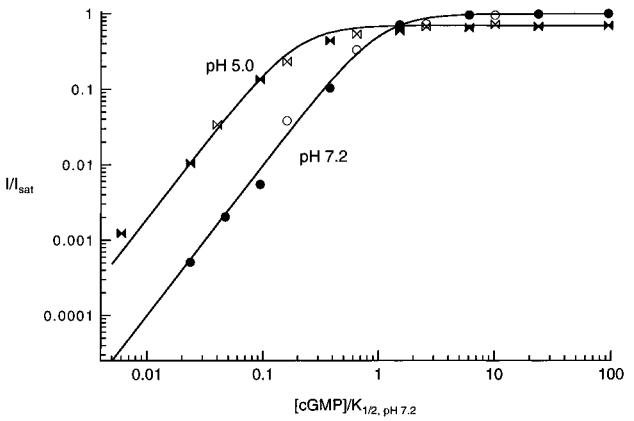


FIGURE 2: Effect of protons on the dose−response curves for activation by cGMP of channels with (wt) and without (H420Q) the $Ni^{2+}$-binding site. To compare apparent affinities with patches that contained amino acid substitutions, the Hill equation was normalized by $K_{1/2,\ pH\ 7.2}$. Therefore, cGMP concentration divided by $K_{1/2,\ pH\ 7.2}$ is plotted on the abscissa. The data were normalized by $I_{sat}$ to control for patch-to-patch variability in the number of channels. The solid symbols are from wild-type channels (the same patch as in Figure 1), and the open symbols are from H420Q,A483V channels. The circles were recorded at pH 7.2, and the bows were recorded at pH 5.0. Currents were measured at +100 mV. The curves are fits to the data with the Hill equation, using the following parameters. For the circles, $I_{sat} = 1$ and $n = 2$; and for the bows, $I_{sat} = 0.7$, $K_{1/2,\ pH\ 7.2}/K_{1/2,\ pH\ 5.0} = 5$, and $n = 2$. The unnormalized values for wild type were $K_{1/2,\ pH\ 7.2} = 85\ \mu M$, $K_{1/2,\ pH\ 5.0} = 17\ \mu M$, $I_{sat,\ pH\ 7.2} = 17\,896$ pA, and $I_{sat,\ pH\ 5.0} = 11\,833$ pA. The unnormalized values for H420Q were $K_{1/2,\ pH\ 7.2} = 200\ \mu M$, $K_{1/2,\ pH\ 5.0} = 50\ \mu M$, $I_{sat,\ pH\ 7.2} = 1400$ pA, and $I_{sat,\ pH\ 5.0} = 1000$ pA.

$N = 4$). At saturating cGMP (Figure 1, middle), increasing the proton concentration produced a reversible decrease in the magnitude of the current. At pH 5.0, the current at saturating cGMP was decreased by 30% (±15%, $N = 6$). We did not study this decrease in current; others have previously suggested a block by intracellular protons of native photoreceptor channels (Liebman et al., 1984; Tanaka, 1993).

Dose−response curves at pH 7.2 (solid circles) and 5.0 (solid bows) are shown in Figure 2. The cGMP concentrations used to elicit the current were normalized by $K_{1/2,\ pH\ 7.2}$ to facilitate comparison with a mutant channel (see below; Zimmerman & Baylor, 1986). As predicted, decreasing the pH shifted the curve to the left, increasing the fraction of current activated by low cGMP concentrations. The solid curves shown in Figure 2 are fits to the data with the Hill equation (see Materials and Methods) in which $K_{1/2,\ pH\ 7.2}/K_{1/2,\ pH\ 5.0} = 5$. For six patches examined, the $K_{1/2}$ decreased from 78.2 $\mu$M (±16.4 $\mu$M) at pH 7.2 to 17.2 $\mu$M (±6.71 $\mu$M) at pH 5.0.

The increase in the relative magnitude of the current activated by saturating cAMP presents an important clue to understanding the mechanism of potentiation by protons. As discussed above, channels open poorly when cAMP is bound because a cAMP-bound channel cannot efficiently undergo the allosteric transition from the closed to the open configuration. The increase in the number of channels activated at low pH by saturating cAMP, with respect to saturating cGMP, must therefore result from an increased ability of cAMP to promote the allosteric transition. To understand the mechanism of potentiation by protons, we have used the following model, similar to that proposed by Karpen et al. (1988), to describe CNG channel behavior (Gordon & Zagotta, 1995a):

Scheme 1

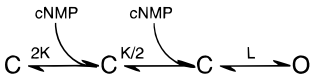


In this model, a channel in the closed configuration is represented by C and a channel in the open configuration is represented by O. Two cyclic nucleotide-binding steps are shown because the Hill coefficient of the dose−response relation was measured to be about 2 (see Figure 2). The ligand binding sites are assumed to be identical and independent, with the equilibrium constant for the initial binding of ligand to the channel equal to $K$. The cyclic nucleotide-binding steps are followed by an allosteric transition to the open configuration, which occurs with an equilibrium constant $L$. When $L$ is large, the free energy difference between the open and closed configurations ($\Delta G_{cNMP}$) of the channel will be negative, and opening will be favored (as with cGMP-bound channels). When $L$ is small, $\Delta G_{cNMP}$ will be less favorable, reducing channel open probability (as with cAMP-bound channels). Although this model clearly cannot account for all channel behavior, including unliganded openings and subconductance states, it can adequately describe channel ligand dependence and gating (Gordon & Zagotta, 1995a; Karpen et al., 1988).

To fit the data with Scheme 1, it was necessary to determine the current attainable at maximal activation of the channels in a patch ($I_{max}$). Note that, in this context, activation refers to the sequence of transitions leading directly to channel opening. Therefore, at maximal activation, the open probability may be less than 1, due to closed states not directly in the activation pathway. We estimated $I_{max}$ as the current at saturating cGMP, in the presence of $Ni^{2+}$ (either 1 or 10 $\mu$M), at the appropriate pH (either 7.2 or 5.0). $Ni^{2+}$ has previously been shown to produce near maximal activation of currents elicited by saturating cGMP in rod channels (Gordon & Zagotta, 1995a). Scheme 1 was fit to the data using $I_{max}$ as obtained by the above method, and the best value for $L_{cGMP}$ was determined. $L_{cAMP}$ was calculated either from fitting the dose−response curves with Scheme 1 or from the value of the current at a saturating cAMP concentration using the following relation derived from Scheme 1:

$$L_{cAMP} = \frac{I_{cAMP}/I_{max}}{1 - I_{cAMP}/I_{max}}$$

The free energy difference between the open and closed configurations of the channel was calculated as $\Delta G = -RT \ln(L_{cNMP})$. Note that this is the free energy difference of channel opening, and not of ligand binding.

One physical mechanism for a proton-induced increase in favorability of $\Delta G_{cNMP}$ would be if protons bound much better to open channels than to closed channels. If protons were more likely to bind to a channel that was open, then a channel that has bound a proton would be more likely to be open. Formalization of preferential binding of protons to the open configuration gives the following model:

Scheme 2

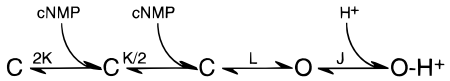

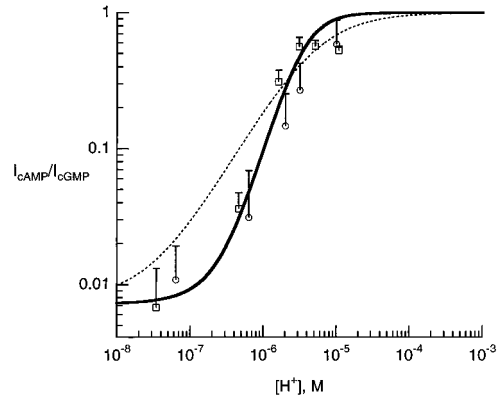


FIGURE 3: Dependence of potentiation on proton concentration. The proton concentration is plotted on the abscissa, and the current in response to 16 mM cAMP normalized to the current at 8 mM cGMP is plotted on the ordinate. The squares represent wild-type channels and the circles A483V channels. The points are means plus standard deviations (bars) of five patches for wild type and six for A483V. Currents were measured at +100 mV. The dotted curve is a fit to the data with Scheme 2, and the solid curve is a fit to the data with scheme 3, both with $L = 0.0072$ (the mean value for five patches), and $J = 3 \times 10^7$ $M^{-1}$ for the dotted curve and $J = 3.5 \times 10^6$ $M^{-1}$ for the solid curve.

Here, $K$ and $L$ have the same meaning as in Scheme 1 and $J$ represents the equilibrium constant for the binding of a proton. While the binding of protons to the channel closed configurations may occur, it must occur with a substantially lower affinity in order for potentiation to be observed. The exclusion of proton-bound closed configurations will cause the model to underestimate how well protons bind to the open configuration; if there were closed configuration binding to overcome, protons would have to bind even better to the open configuration to produce a given amount of potentiation.

The dependence of potentiation on proton concentration was examined to gain information on the number and type(s) of titratable group(s) involved. We measured the magnitude of the current activated by saturating cAMP, relative to that activated by saturating cGMP, at different proton concentrations (Figure 3). Increasing the proton concentration increased the magnitude of potentiation within the pH range examined here (from pH 7.5 to 4.8). Using Scheme 2 to fit the pH dependence data produced the dotted curve shown in Figure 3. The poor fit of Scheme 2 to the data arises from the assumption of a single proton binding site, which yields a curve that is too shallow. Proposing a second proton binding site adds a further state to the model:

Scheme 3

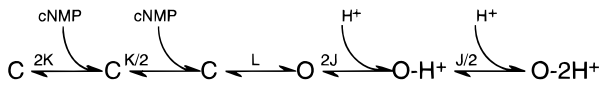


For this scheme, we have assumed the two proton binding sites are equivalent and independent, with the equilibrium constant for the binding of a proton to either site equal to $J$. Fitting the data with Scheme 3 (solid curve) produced an equilibrium constant $J = 3.5 \times 10^6$ $M^{-1}$, equivalent to a $pK_a$ of 6.5. Although the binding sites need not be independent or identical, the approximation of the data by the model suggests that there are at least two sites on the channel to which protons can bind. These could be either equivalent sites on different subunits or sites formed by different regions of the same subunit (see below). Note that Schemes 2 and 3 reduce to Scheme 1, at a fixed proton concentration, if all the open states are aggregated into a single open state, and potentiation is viewed simply as increasing the stability of the open configuration with respect to the closed configuration (decreasing $\Delta G$).

Because divalent transition metal cations, including $Ni^{2+}$, also increase the maximum current in response to cAMP and increase the apparent affinity for cGMP (Gordon & Zagotta, 1995a; Ildefonse et al., 1992; Karpen et al., 1993), we explored the possibility that $Ni^{2+}$ and protons work through a common site of action. The binding site for potentiation by $Ni^{2+}$ has previously been shown to include a single histidine residue (H420) in the intracellular region of the channel following the sixth transmembrane domain. The preferential binding of $Ni^{2+}$ to the open state of the channel could account for the increases in the apparent affinity of the channels for cGMP and cAMP, and in the maximum current activated by cAMP. Mutation of this histidine to a glutamine (H420Q) completely eliminated the ability of $Ni^{2+}$ to potentiate the channels (Gordon & Zagotta, 1995a). We studied the effects of lowering pH on channels containing the H420Q mutation to see if they could still be potentiated by protons. The results of one such comparison are shown in Figure 2. Here, data from the wild-type channels are shown as solid symbols and data from the H420Q channels are shown as open symbols. Data obtained at pH 7.2 are shown as circles, and data obtained at pH 5.0 are shown as bows. For the four H420Q patches examined, the $K_{1/2}$ for activation by cGMP was 6.9-fold ($\pm 1.9$, $N = 4$) lower at pH 5.0 than at pH 7.2. This is comparable to the 5.0-fold ($\pm 2$, $N = 6$) decrease in $K_{1/2}$ measured for wild-type channels. The lack of attenuation of potentiation in H420Q channels indicates that the histidine required for $Ni^{2+}$ potentiation is not likely to play a role in potentiation by protons.

Comparison of the degree of potentiation observed with protons to that observed with $Ni^{2+}$ revealed a difference in the cyclic nucleotide dependence of these two factors. While $Ni^{2+}$ potentiated cAMP- and cGMP-bound channels to a similar extent, protons potentiated cAMP-bound channels more than cGMP-bound channels. Shown in Figure 4A are currents in response to saturating cAMP both with and without 10 $\mu$M $Ni^{2+}$ (a concentration which gives maximal potentiation) and at high and low pH. The currents were normalized to $I_{max}$, at the same pH, so that the magnitude of the normalized current reflects the fraction of the channels activated by cAMP (see Materials and Methods). This type of comparison shows that, while 10 $\mu$M $Ni^{2+}$ increased the fraction of channels activated by cAMP about 50-fold, 10 $\mu$M protons increased the fraction of channels activated by cAMP about 100-fold. The dose−response curves for activation of the channels by cGMP (Figure 4B) demonstrate that the efficacies of $Ni^{2+}$ and protons on cGMP-bound channels were reversed compared to their efficacies on cAMP-bound channels. In case of cGMP, $Ni^{2+}$ (solid circles) was more effective than protons (open circles), shifting the dose−response curve further to the left. The solid curves shown are fits to the data with Scheme 1. From these fits and the cAMP data in Figure 4A, we calculated the difference between $\Delta G$ of the potentiated and unpotentiated channels for cAMP and cGMP. These data are shown for protons and $Ni^{2+}$ in Figure 4C. Whereas $Ni^{2+}$ increased

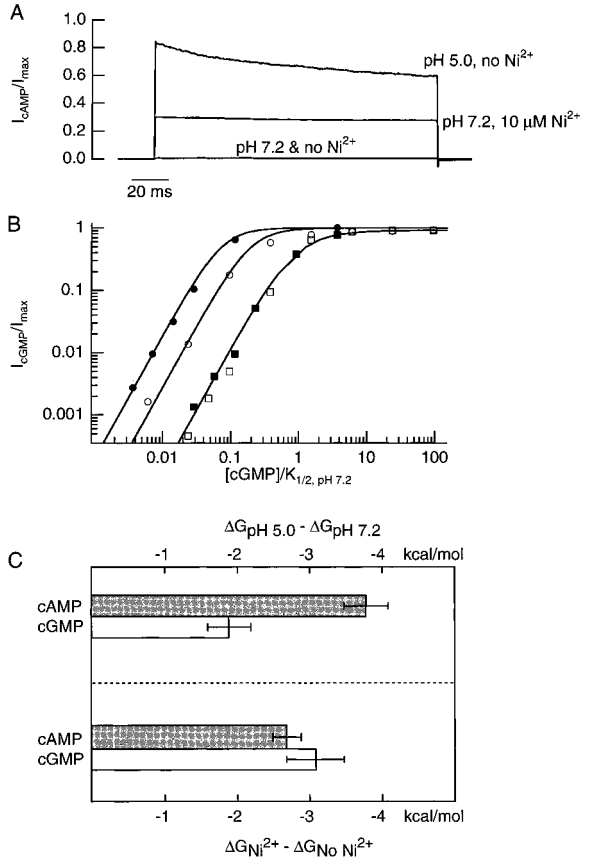


FIGURE 4: Nucleotide dependence of potentiation. (A) Protons potentiate cAMP-bound channels more than does $Ni^{2+}$. Currents in response to voltage pulses from a holding potential of 0 to +100 mV, in the presence of 16 mM cAMP. Currents were from two different patches, one which was exposed to low pH, and a second which was exposed to $Ni^{2+}$. The currents were normalized to the value of the current for each patch at saturating cGMP and 10 $\mu$M $Ni^{2+}$, measured at the same pH. The bottom line contains two overlapping traces, one trace for each patch, measured at pH 7.2 and no $Ni^{2+}$. (B) Dose−response curves for activation by cGMP of wild-type channels, at pH 7.2 (open squares) and pH 5.0 (open circles), and of A483V channels in the absence (solid squares) and presence (solid circles) of 10 $\mu$M $Ni^{2+}$. The data for each type of experiment (pH or $Ni^{2+}$) are from the same patches as shown in panel A. The data were normalized to $I_{max}$ (see text) with $I_{max}$ = 19 744 pA for the pH 7.2 curve, $I_{max}$ = 13 599 pA for the pH 5.0 curve, and $I_{max}$ = 18 927 pA for the $Ni^{2+}$ experiment. The concentrations were normalized to the $K_{1/2, pH 7.2}$ for each patch, with $K_{1/2}$ = 141 $\mu$M for the $Ni^{2+}$ experiment and $K_{1/2}$ = 85 $\mu$M for the pH experiment. The solid lines are fits to the data with Scheme 1. For no Ni, pH 7.2, $L$ = 11, and $K$ = 3941 $M^{-1}$ for the pH experiment and $L$ = 11, and $K$ = 2376 $M^{-1}$ for the $Ni^{2+}$ experiment. For the pH 5.0 curve, $L$ = 250, and $K$ = 3941 $M^{-1}$, and for the 10 $\mu$M $Ni^{2+}$ curve, $L$ = 1700, and $K$ = 2376 $M^{-1}$. (C) Difference in the free energy difference between the open and closed configurations at pH 5.0 and 7.2 (upper) and 10 $\mu$M $Ni^{2+}$ and no $Ni^{2+}$ (lower). The bars represent standard deviations. Shaded columns were calculated from data at 16 mM cAMP, and open columns were obtained from fits to dose−response curves for cGMP.

the stability of the allosteric transition from the closed to the open configurations to a similar extent for cAMP- and cGMP-bound channels, protons increased its stability more for cAMP- than for cGMP-bound channels. The unequal effects of protons on cAMP-bound and cGMP-bound channels explain why protons potentiated cAMP-bound channels more effectively than did $Ni^{2+}$ but potentiated cGMP-bound channels less effectively than did $Ni^{2+}$.

The ability of protons to potentiate cAMP-bound channels more than cGMP-bound channels suggests that the proton

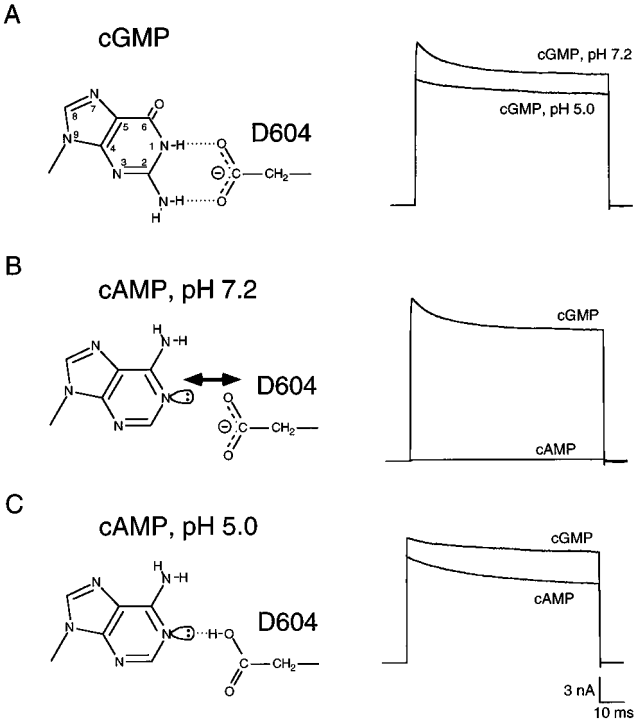


FIGURE 5: Molecular basis for ligand specificity of proton effects. The panels on the left are representations of the cyclic nucleotide purine ring interactions with D604. The panels on the right are from the currents shown in Figure 1 and are all shown on the same scale (see scale bars below). (A) N1 and N2 groups of cGMP form hydrogen bonds with carboxyl group oxygens of D604. (B) Unfavorable interaction between unshared electrons in the $sp^2$ orbital of N1 nitrogen on cAMP and negatively charged D604. (C) A proton stabilizes the cAMP−D604 interaction by buffering the electronegativity of the unshared electrons at N1 of cAMP.

binding sites might involve an amino acid residue(s) that interacts differently with cAMP than with cGMP. One such residue is D604, located in the putative C α-helix of the cyclic nucleotide-binding domain. D604 has recently been shown to interact favorably with bound cGMP, resulting in strong channel activation, and interact unfavorably with bound cAMP, resulting in its partial agonist behavior (Varnum et al., 1995). These interactions occur only when the channel is open, accounting for the difference in the free energy of the allosteric transition between cAMP ($\Delta G_{cAMP}$) and cGMP ($\Delta G_{cGMP}$). A molecular interpretation of the effects of protons on these interactions is shown in Figure 5. For cGMP, the negatively charged carboxylate group of D604 forms a pair of hydrogen bonds with N1 and N2 of the guanine ring; protons are not expected to perturb this specific and energetically favorable interaction (Figure 5A). As shown in Figure 5B, the negative charge of D604 would present an unfavorable electrostatic interaction with the unshared pair of electrons in the $sp^2$ orbital at N1 of cAMP. Protonation of D604 could relieve some of this unfavorable interaction. Although interaction of a proton with a free aspartic acid residue usually occurs with a p$K_a$ of about 4 (Creighton, 1993), the sharing of a proton between D604 and N1 of cAMP (Figure 5C) would be expected to occur with a much higher p$K_a$. Significant proton binding would occur only when two conditions are met: (1) cAMP is bound to the channels and (2) the channels are open.

If protonation of D604 contributes to potentiation of cAMP-bound but not cGMP-bound channels, then elimination of the negative charge at the 604 position should

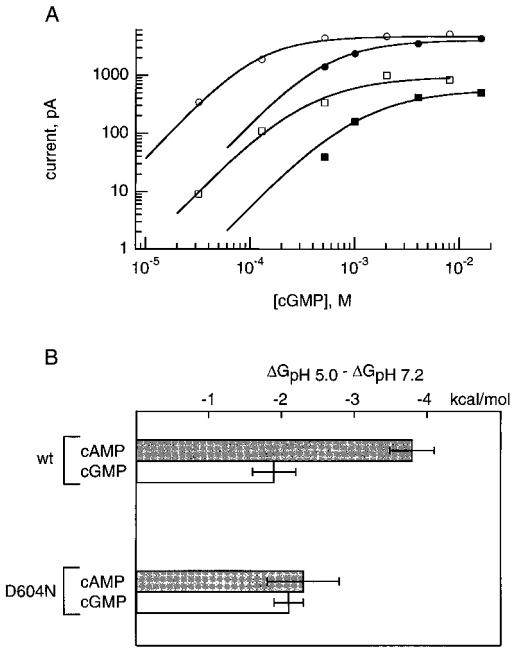


FIGURE 6: Elimination of the cAMP-specific component of potentiation by removal of the protonatable group at D604. (A) Dose−response curves for activation of the channels by cGMP (open symbols) and cAMP (filled symbols) at pH 7.2 (squares) and pH 5.0 (circles). Currents were measured at +100 mV. The solid curves are fits to the data with scheme 1 with the following parameters. For cGMP, $L = 0.16$, $K = 3224$ M$^{-1}$, and $I_{max} = 6999$ pA for pH 7.2 and $L = 7$, $K = 3224$ M$^{-1}$, and $I_{max} = 5471$ pA for pH 5.0. For cAMP, $L = 0.091$, $K = 1013$ M$^{-1}$, and $I_{max} = 6999$ pA for pH 7.2 and $L = 3.2$, $K = 1013$ M$^{-1}$, and $I_{max} = 5471$ pA for pH 5.0 (B) Difference in the free energy difference between the open and closed configurations between channels at pH 5.0 and 7.2.

diminish proton potentiation of cAMP-bound channels but not cGMP-bound channels. This prediction is borne out, as demonstrated by the data shown in Figure 6 using channels in which D604 was replaced by asparagine (D604N). D604N is especially interesting because subunit 2 of the human rod channel contains asparagine at the position corresponding to 604. Dose−response curves for cGMP and cAMP are shown in Figure 6A. D604N channels were not activated by cGMP as well as were wild-type channels (Varnum et al., 1995) because the favorable carboxylate−cGMP interactions have been diminished. Furthermore, cAMP activated a larger fraction of the current at pH 7.2 than in the wild type, due to the removal of the unfavorable electrostatic interaction (compare with the bottom trace of Figure 4A; Varnum et al., 1995). For D604N, going from pH 7.2 (squares) to pH 5.0 (circles) caused an increase in the apparent affinity and maximum current for both cGMP (open symbols) and cAMP (filled symbols). The solid curves in the figure are fits to the data with Scheme 1. These fits gave a change in the free energy difference between the open and closed configurations that was comparable for cAMP- and cGMP-bound channels (Figure 6B). Replacing the aspartic acid residue with asparagine thus removed the potentiation specific to cAMP-bound channels without altering potentiation of cGMP-bound channels. These results suggest that the reduced proton potentiation observed in native channels (Sanfilippo & Menini, 1993) may have been due to the asparagine present at the position corresponding to 604 in subunit 2 (see below).

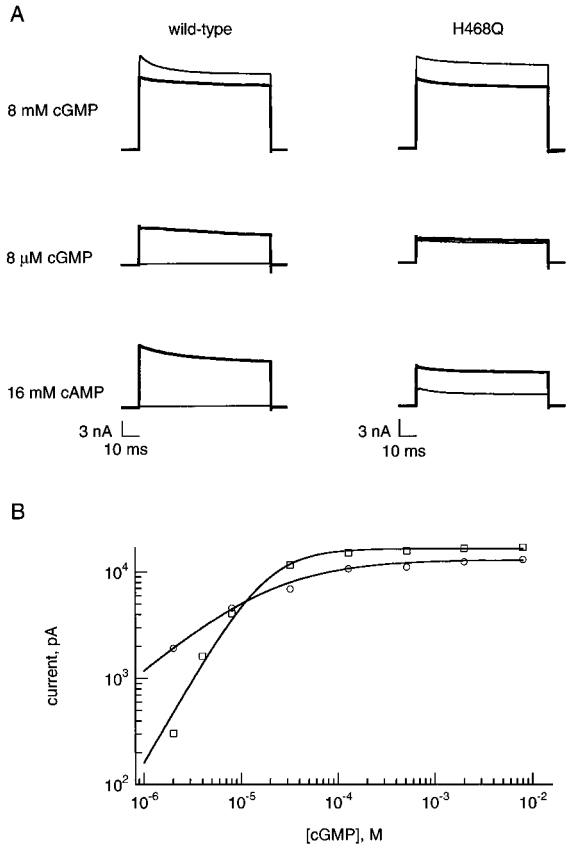


FIGURE 7: Potentiation was attenuated in H468Q. (A) Currents for wild type (left) and H468Q (right) in response to voltage steps from a holding potential of 0 to +100 mV. Thick lines were recorded at pH 5.0, and thin lines were recorded at pH 7.2. Each patch (wild type or H468Q) has its own scale bar. (B) Dose−response curves for activation of H468Q by cGMP at pH 7.2 (squares) and pH 5.0 (circles), from the patch shown in panel A. The solid curves are fits to the data with the Hill equation using the following parameters. For pH 7.2, $I_{sat} = 16\,500$ pA, $K_{1/2} = 18$ $\mu$M, and $n = 1.6$; for pH 5.0, $I_{sat} = 13\,000$ pA, $K_{1/2} = 18$ $\mu$M, and $n = 0.8$. Currents were measured at +100 mV.

Although elimination of proton binding at the 604 position by introduction of the D604N mutation removed the cAMP-specific component of proton potentiation, a nucleotide-nonspecific component of potentiation by protons remained. Because the p$K_a$ of proton binding was in the range normally observed for protonation of histidine residues, we examined the effect of mutating histidine residues on proton potentiation. As shown earlier, H420Q still exhibited a normal degree of potentiation of cGMP-bound channels. However, we found that mutation of the histidine at position 468 to a glutamine (H468Q) appeared to attenuate proton potentiation in both cGMP- and cAMP-bound channels. The results from one such experiment are shown in Figure 7. Currents recorded at pH 7.2 are shown with thin lines, and those recorded at pH 5.0 are shown with thick lines (Figure 7A). The currents in response to 8 mM cGMP (top panel) were comparable in wild type (left) and H468Q (right) at high and low pH. H468Q differed from wild type in that it was activated better by both cGMP and cAMP, even at pH 7.2 (note the higher apparent affinity for cGMP and the greater fractional activation by cAMP compared to those of wild type). Furthermore, the degree of potentiation observed at 8 $\mu$M cGMP (middle panel) and 16 mM cAMP (bottom panel) was smaller in H468Q than in wild-type channels. Using Scheme 1, $\Delta G_{cAMP}$ (pH 5.0) − $\Delta G_{cAMP}$ (pH 7.2) was

calculated to equal −1.1 kcal/mol (±0.25, $N = 6$). Dose−response curves for activation of H468Q by cGMP at pH 7.2 (squares) and pH 5.0 (circles) revealed a complicating factor in the effects of protons on this channel type. The currents obtained from H468Q channels were not as steeply dependent on cGMP concentration as those of wild-type channels. Although we did not study this phenomenon in detail, the shallow slope of the relation at pH 5.0 prevents scheme 1 from being used to fit the potentiation observed in cGMP-bound channels.

If protonation at D604 accounts for the cAMP-specific component of potentiation and H468 accounts for a nucleotide-nonspecific component of potentiation, then a channel that contains both the D604N and the H468Q mutations should exhibit little or no potentiation by protons. We were unable to test this hypothesis because these double-mutant channels did not express. However, subunit 2 of the rod channel contains asparagines at both of these positions (Chen et al., 1993). Subunit 2 does not express by itself but can be examined by coexpression with subunit 1. Channels with some subunits containing both protonatable sites (subunit 1) and some subunits containing neither protonatable site (subunit 2) would be expected to exhibit decreased potentiation by protons of both cAMP and cGMP activation. The results of coinjection of RNA from subunits 1 and 2 are shown in Figure 8. Although both cAMP-bound (Figure 8A) and cGMP-bound (Figure 8B) channels still exhibited potentiation, fitting the data with Scheme 1 demonstrated that the degree of potentiation was reduced compared to that of wild type (Figure 8C). Furthermore, since the fraction of channels that incorporated subunit 2 is unknown, some or all of the observed potentiation may have been due to channels formed exclusively from subunit 1. Thus, the absence of protonatable groups at the positions corresponding to 468 and 604 can account for at least part of the reduced proton potentiation reported for native rod channels (Sanfilippo & Menini, 1993).

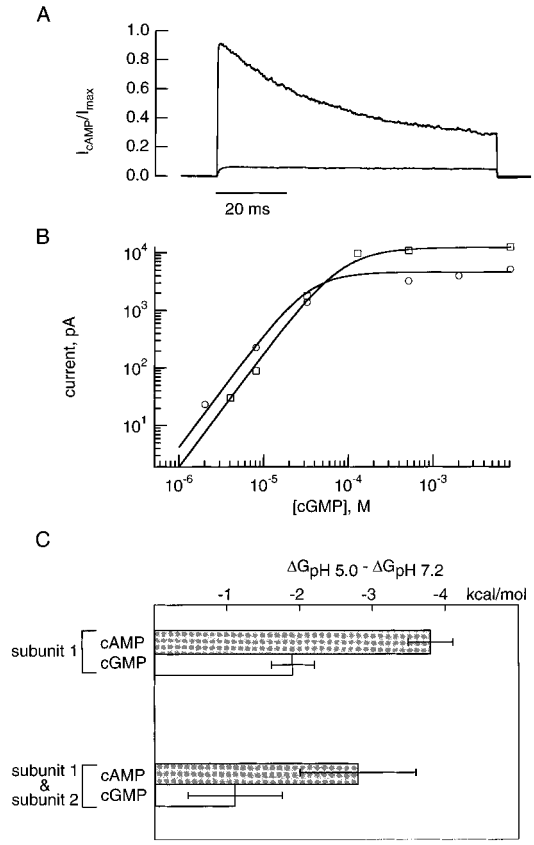


FIGURE 8: Reduced potentiation in channels formed from both subunit 1 and subunit 2. (A) Currents at 16 mM cAMP in response to voltage steps from a holding potential of 0 to +100 mV at pH 7.2 (lower trace) and pH 5.0 (upper trace). Currents were normalized to the maximum current in saturating cGMP and 10 $\mu$M $Ni^{2+}$, at the appropriate pH. (B) Dose−response curves for activation of the channels by cGMP at pH 7.2 (squares) and pH 5.0 (circles), for the patch shown in panel A. The solid curves are fits to the data with scheme 1, with $I_{max} = 13\,378$ pA, $K = 3000$ $M^{-1}$, and $L = 16$ at pH 7.2 and $I_{max} = 4705$ pA, $K = 3000$ $M^{-1}$ and $L = 100$ at pH 5.0. Currents were measured at +100 mV. (C) Difference in the free energy difference between the open and closed configurations between channels at pH 5.0 and 7.2.

## DISCUSSION

In this paper, we have characterized potentiation of rod CNG channels by protons. We found that cAMP-bound channels were potentiated more than were cGMP-bound channels. The cAMP-specific component of potentiation appeared to be due to protonation at D604, which removed an unfavorable interaction between the carboxylate of D604 and the purine ring of cAMP. These experiments provide another line of evidence implicating D604 as a major element in the coordination of cyclic nucleotide binding and channel opening. At least one more amino acid, H468, contributed to potentiation for both cAMP and cGMP. H468 is located in an intracellular region of the channel between the sixth transmembrane segment and the cyclic nucleotide-binding domain, a region thought to be important for channel gating (Gordon & Zagotta, 1995a,b). Our results suggest that H468 may have a role in the channel activation process.

The model which best fit the pH dependence of potentiation for cAMP (Scheme 3) involved the binding of protons to two sites. Although we invoked two identical, independent sites, we cannot exclude the possibility of nonidentical and/or nonindependent sites. In this paper, we have described two amino acids, D604 and H468, whose protonation appeared to contribute to potentiation of the channels. These two amino acids are obvious candidates for the sites. Alternatively, the two main sites titrated in the proton concentration range examined here could be the same amino acid, such as D604, on different subunits of the channel. This type of scenario has been found to be the case for the binding of protons to glutamate residues near the outer mouth of the channel pore (Root & MacKinnon, 1994). The issue of the physical basis of the sites raises several questions. How many subunits must have protonated amino acids in order to produce potentiation? Does potentiation incrementally increase as the number of protonated subunits/residues increases? And are there proton binding sites other than the two identified here?

The results we report here may explain the effects of intracellular protons on native photoreceptor channels. In the native channels, protons were found to increase the maximum current and apparent affinity of cAMP-bound channels but did not potentiate cGMP-bound channels (Sanfilippo & Menini, 1993). Native photoreceptor channels are composed of at least two subunits, with unknown stoichiometry (Chen et al., 1993). Instead of a histidine and an aspartic acid residue, like subunit 1, subunit 2 contains an asparagine residue at the positions corresponding to 468

and 604. The presence of subunit 2 in the channel complex, in and of itself, is sufficient to make the channels activated better by cAMP than channels composed of just subunit 1 (compare Figure 8A to Figure 4A; Fodor & Zagotta, 1996). As predicted, channels formed by coinjection of RNA from subunits 1 and 2 exhibited less potentiation than channels formed exclusively from subunit 1. These results suggest that the existence of two fewer protonatable sites on subunit 2 accounts for the reduced potentiation observed in native channels.

Do increases in intracellular pH play a role in ion channel modulation *in vivo*? Protons, a product of cGMP hydrolysis, have been found to relieve $Ca^{2+}$ block of the channels (Tanaka, 1993), and extracellular protons have been found to decrease the photoreceptor dark current (Liebman et al., 1984) and the conductance of the channels by binding to glutamate residues near the extracellular mouth of the channel pore (Root & MacKinnon, 1994). Although not enough is known about pH fluctuations and cAMP concentration in photoreceptor cells to assess the importance of pH changes in visual transduction, a role for pH changes in modulation of related CNG channels in sperm (Weyand et al., 1994) and pinealocytes (Distler et al., 1994; Dryer & Henderson, 1991) can be imagined. In both these cell types, changes in intracellular pH are thought to accompany activation (via contact with egg peptides in sperm and via sympathetic innervation in pinealocytes). Whether these changes in intracellular pH influence to what extent the channels open and/or to which cyclic nucleotide they respond remains to be determined.

## ACKNOWLEDGMENT

We thank Kevin Black, Lorie Devlin, and Gay Sheridan for excellent technical assistance and Drs. Jeffrey W. Karpen and Anita L. Zimmerman for comments on the manuscript. In addition, we thank E. R. Liman for the high-expression vector and K.-W. Yau for the subunit 2 cDNA. This work was supported by a grant from the National Eye Institute (EY10329 to W.N.Z.) and the Human Frontier Science Program. W.N.Z. is an Investigator and S.E.G. and M.D.V. are Associates of the Howard Hughes Medical Institute.

## REFERENCES

Bradley, J., Li, J., Davidson, N., Lester, H. A., & Zinn, K. (1994) *Proc. Natl. Acad. Sci. U.S.A. 91*, 8890−4.

Chen, T. Y., Peng, Y. W., Dhallan, R. S., Ahamed, B., Reed, R. R., & Yau, K. W. (1993) *Nature 362*, 764−7.

Creighton, T. E. (1993) *Proteins: structures and molecular properties*, 2nd ed., W. H. Freeman and Company, New York.

Distler, M., Biel, M., Flockerzi, V., & Hofmann, F. (1994) *Neuropharmacology 33*, 1275−82.

Dryer, S. E., & Henderson, D. (1991) *Nature 353*, 756−8.

Fodor, A. A., & Zagotta, W. N. (1996) *Biophys. J. 70*, 368a.

Gordon, S. E., & Zagotta, W. N. (1995a) *Neuron 14*, 177−83.

Gordon, S. E., & Zagotta, W. N. (1995b) *Neuron 14*, 857−64.

Goulding, E. H., Ngai, J., Kramer, R. H., Colicos, S., Axel, R., Siegelbaum, S. A., & Chess, A. (1992) *Neuron 8*, 45−58.

Hamill, O. P., Marty, A., Neher, E., Sakmann, B., & Sigworth, F. J. (1981) *Pfluegers Arch. 391*, 85−100.

Ildefonse, M., Crouzy, S., & Bennett, N. (1992) *J. Membr. Biol. 130*, 91−104.

Karpen, J. W., Zimmerman, A. L., Stryer, L., & Baylor, D. A. (1988) *Proc. Natl. Acad. Sci. U.S.A. 85*, 1287−91.

Karpen, J. W., Brown, R. L., Stryer, L., & Baylor, D. A. (1993) *J. Gen. Physiol. 101*, 1−25.

Kaupp, U. B., Niidome, T., Tanabe, T., Terada, S., Bonigk, W., Stuhmer, W., Cook, N. J., Kangawa, K., Matsuo, H., Hirose, T., Miyata, T., & Numa, S. (1989) *Nature 342*, 762−6.

Lagnado, L., & Baylor, D. (1992) *Neuron 8*, 995−1002.

Liebman, P. A., Mueller, P., & Pugh, E. N. J. (1984) *J. Physiol. (London) 347*, 85−110.

Liman, E. R., & Buck, L. B. (1994) *Neuron 13*, 611−21.

Liman, E. R., Tytgat, J., & Hess, P. (1992) *Neuron 9*, 861−71.

Root, M. J., & MacKinnon, R. (1994) *Science 265*, 1852−6.

Sanfilippo, C., & Menini, A. (1993) *Biophys. J. 64*, A17.

Su, Y., Dostmann, W. R. G., Herberg, F. W., Durick, K., Xuong, N.-h., Ten Eyck, L., Taylor, S. S., & Varughese, K. I. (1995) *Science 269*, 807−13.

Takio, K., Smith, S. B., Krebs, E. G., Walsh, K. A., & Titani, K. (1984) *Biochemistry 23*, 4200−6.

Tanaka, J. C. (1993) *Biophys. J. 65*, 2517−23.

Varnum, M. D., Black, K. D., & Zagotta, W. N. (1995) *Neuron 15*, 619−25.

Weber, I. T., & Steitz, T. A. (1987) *J. Mol. Biol. 198*, 311−26.

Weyand, I., Godde, M., Frings, S., Weiner, J., Muller, F., Altenhofen, W., Hatt, H., & Kaupp, U. B. (1994) *Nature 368*, 859−63.

Zagotta, W. N., Hoshi, T., & Aldrich, R. W. (1989) *Proc. Natl. Acad. Sci. U.S.A. 86*, 7243−7.

Zimmerman, A. L., & Baylor, D. A. (1986) *Nature 321*, 70−2.

Zimmerman, A. L., Karpen, J. W., & Baylor, D. A. (1988) *Biophys. J. 54*, 351−5.

BI952607B